ACS Macro Letters

Letter

pubs.acs.org/macroletters

Atomic Force Microscopy Nanomechanics Visualizes Molecular Diffusion and Microstructure at an Interface

Dong Wang,*[,†] Thomas P. Russell,[†,‡] Toshio Nishi,[†] and Ken Nakajima[†]

[†]WPI−Advanced Institute for Materials Research (WPI-AIMR), Tohoku University, 2-1-1 Katahira, Aoba, Sendai 980-8577, Japan

[‡]Department of Polymer Science and Engineering, University of Massachsetts, Amherst, Massachusetts 01003, United States

Supporting Information

ABSTRACT: Here we demonstrate a simple, yet powerful method, atomic force microscopy (AFM) nanomechanical mapping, to directly visualize the interdiffusion and microstructure at the interface between two polymers. Nanomechanical measurements on the interface between poly(vinyl chloride) (PVC) and poly(caprolactone) (PCL) allow quantification of diffusion kinetics, observation of microstructure, and evaluation of mechanical properties of the interdiffusion regions. These results suggest that nanomechanical mapping of interdiffusion enables the quantification of diffusion with high resolution over large distances without the need of labeling and the assessment of mechanical property changes resulting from the interdiffusion.

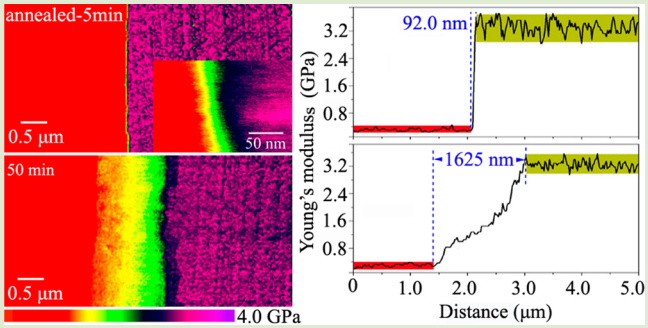

Techniques to detect and study diffusion and microstructure at an interface have played a central role in various processings of materials technologies.[1−6] Over the past decades, several techniques have been developed, such as forward recoil spectroscopy (FRES), dynamic secondary ion mass spectroscopy (DSIMS), neutron scattering, or neutron reflectivity, to quantify concentration profiles at buried interfaces.[7−20] In general each requires the selective labeling of one of the components, and none can simultaneously provide information related to the microstructure and mechanical properties within an interfacial region, which can be important for the ultimate properties of a material.

Recently developed atomic force microscopy (AFM) nanomechanical measurements, such as force volume (FV),[21−23] harmonic force microscopy,[24] band excitation methods,[25] and contact resonance based techniques,[26] have become simple and efficient methods to obtain the elastic and adhesive properties of materials with surface heterogeneities. In the present work, by exploiting mechanical properties changes accompanying the diffusion of two polymers,[27] we use AFM nanomechanical mapping to investigate interdiffusion of two miscible polymers, poly(vinyl chloride) (PVC) and poly(caprolactone) (PCL).[1,28] The variation in the stiffness in the interfacial regions enables the simultaneous quantification of diffusion kinetics and the characterization of the microstructure and mechanical properties within the concentration gradient between the two polymers.

EXPERIMENTAL SECTION

The bilayer samples were prepared according to ref 28. A brief description is included here: PCL sheets, having a thickness of ∼250 μm and a surface roughness R_q (r.m.s.) of 4.2 nm over 5 × 5 μm^2, were placed on top of the PVC sheets, having a thickness of ∼250 μm and R_q of 1.3 nm over 5 × 5 μm^2. The two sheets were first pressed together by hand (the press does not induce the diffusion, as demonstrated by Macosko[20]) and were then placed in a vacuum oven at temperature above the melting temperature of PCL (T_m = 60 °C) but lower than the T_g (80 °C) of PVC to investigate the diffusion behaviors at a glassy (here is PVC) and rubbery (liquid, here is PCL) interface. Initially, PCL flowed sufficiently to provide excellent contact between the two layers. After a set period of time the samples were quenched in liquid nitrogen to arrest the interdiffusion and freeze-in the morphology. The bilayers were then ultramicrotomed using a Leica EM FC6 at −120 °C to obtain a flat surface for AFM characterization. The cut is normal to the diffusion direction to minimize influence of the interface morphology. Detailed experimental information is provided in the Supporting Information (SI).

Nanomechanical mapping was operated in PeakForce QNM (Quantitative NanoMechanics) mode on a Bruker MultiMode AFM at ambient conditions. The samples were scanned at constant peak force of 20 nN using a rectangular silicon cantilever with nominal spring constant of 25 N/m (OMCL-AC160TS-R3, Olympus Micro Cantilevers). Actual spring constant was measured by a thermal tuning method. The applied force between the tip and sample is designed to be smaller than the yield stress of both PVC (83 MPa, obtained by compression testing[29]) and PCL (22 MPa), and only elastic deformation is involved in the measurement. The oscillation frequency of the Z-piezo was 1 kHz, and the peak force amplitude was the default value of 150 nm. The tip radius was obtained by tapping mode imaging of a Nioprobe tip-check sample and then analyzed by commercial SPIP software. The reduced Young's modulus, E^*, is

Received: June 3, 2013
Accepted: August 2, 2013
Published: August 6, 2013

   dx.doi.org/10.1021/mz400281f | ACS Macro Lett. 2013, 2, 757−760

obtained by fitting the unloading curve using the Derjaguin, Muller, Toropov (DMT) model,[30] which takes into account the adhesive force between the tip and the surface. The DMT theory is expressed by the following equation

$$E^* = \frac{3(F_{tip} - F_{adh})}{4\sqrt{Rd^3}} \quad (1)$$

where F_{tip} is the force on the AFM tip; F_{adh} is the adhesive force; R is the tip radius; and d is the deformation value. E^* is the reduced elastic modulus and has the relationship to sample Young's modulus, E_s, as follows

$$E_s = (1 - \nu_s^2)E^* \quad (2)$$

where ν_s is the sample Poission's ratio. Thus, a combination of eqs 1 and 2 gives E_s.

When the AFM tip presses against the sample surface at a constant force, the cantilever will deflect to higher values in stiffer regions and lower values in softer regions. Figure 1 shows

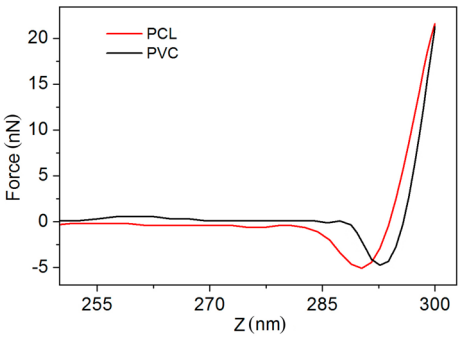

Figure 1. Typical force−Z-piezo displacement curve of PCL and PVC.

two typical force curves corresponding to the PCL and PVC. In the resulting Young's modulus maps shown in Figure 2, red regions with lower Young's modulus are assigned to the PCL, while purple-black regions with higher Young's modulus are assigned to PVC. The histogram in Figure 3 shows statistical results of the Young's modulus for samples annealed for 5 and 50 min. The statistical distribution of the Young's modulus can

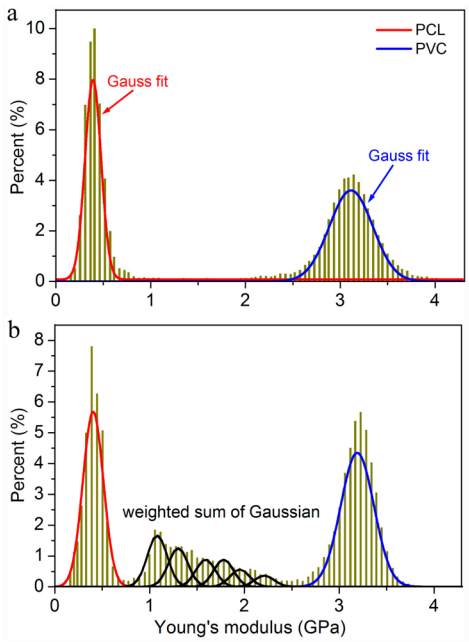

Figure 3. Histograms of nanomechanical mapping. (a), (b) PVC/PCL samples annealed for 5 and 50 min, respectively, corresponding to the image shown in Figure 2 (a) and (c).

be well-described by a Gaussian function with a mean value of 340 ± 38.0 MPa for PCL and 3.2 ± 0.4 GPa for PVC, which are consistent with that of bulk values.[31,32] Thus, the nanomechanical mapping can accurately describe the mechanical properties of these pure components. It should be noted that the variance in both the Young's modulus maps and section profiles in Figure 2 reflects heterogeneities or fluctuations in both glassy PVC and semicrystalline PCL. Our previous work has shown that even in standard glassy polystyrene (PS) there are mechanical heterogeneities that are 2 to 3 nm in size, which can be identified with fluctuations in viscoelastic properties or density fluctuations in the material.[33] PCL, quenched from melt into liquid nitrogen, will partially crystallize after it is brought to

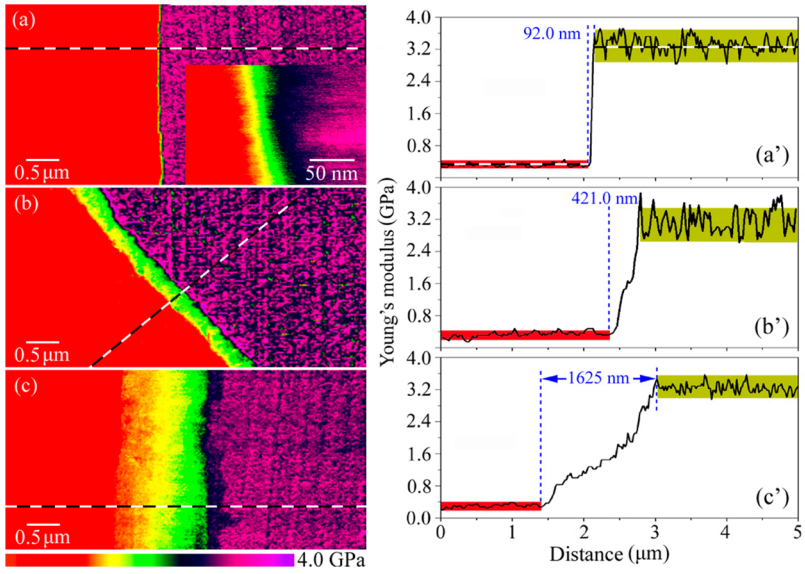

Figure 2. Young's modulus maps of the PVC/PCL sample annealed at 72 °C for (a) 5, (b) 20, and (c) 50 min and corresponding modulus profiles (a'), (b'), and (c') across the interface, respectively. The Young's modulus of PVC and PCL is indicated as a dashed line in (a').

dx.doi.org/10.1021/mz400281f | ACS Macro Lett. 2013, 2, 757−760

room temperature because of its low glass transition temperature (T_g = −60 °C). The coexistence of crystalline and amorphous regions will lead to the variations in the Young's modulus. Other factors, like surface roughness, capillary force, and density fluctuations will also produce a variation in the measured Young's modulus.[34]

Between the two pure layers of PVC and PCL an area with a gradient in the Young's modulus is evident (dark blue to green to yellow), arising from the interdiffusion of the polymers. The histogram in Figure 3b shows a broadening of the modulus distribution in this region that can be fit with a weighted sum of Gaussian distributions and gives a mean Young's modulus of 1.08, 1.30, 1.59, 1.78, 1.95, and 2.21 GPa of the interdiffusion regions. A Young's modulus profile across the diffusion region shows that the transition between the Young's modulus of the two polymers broadens significantly with increasing diffusion time (Figure 2 and Figure S1, SI). The width of this interfacial region is taken as the diffusion length (it was determined using at least 20 single modulus profiles) and can be obtained by measuring the transition distance that the Young's modulus increases from that of PCL to that of PVC. The diffusion length for the sample annealed for 5 min is ∼92.0 nm and after annealing for 20 min increases to ∼421 nm. As shown in Figure 4a the diffusion length increases linearly with time, indicating

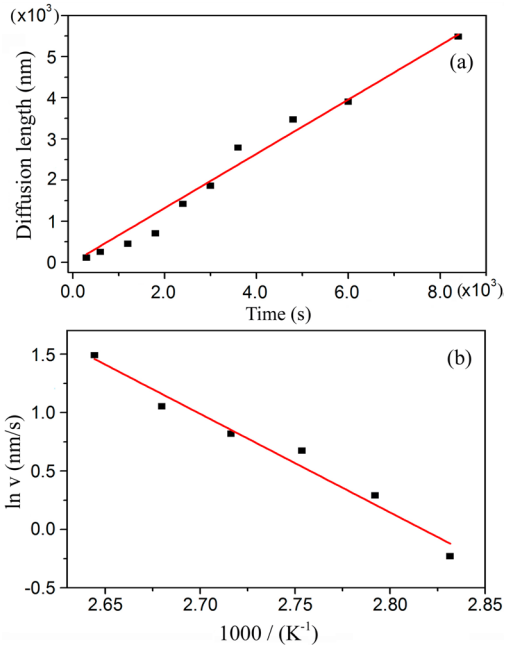

Figure 4. Diffusion kinetics data. (a) Diffusion length vs diffusion time at 72 °C indicates the diffusion rate v of the PCL/PVC interface is approximately constant. (b) ln v vs $1/T$. Slope of the linear least-squares line gives an apparent activation energy for diffusion of 69.8 kcal/mol for the PVC/PCL system.

that the diffusion rate v between the two polymers is roughly constant, similar to that seen with Case-II diffusion.[35−37]

We also directly observed a nonuniformity in the mechanical properties along the diffusion front, as evidenced by the mottled texture in the gradient in the Young's modulus maps at the diffusion front, as seen in the samples annealed for 5 min (the inset in Figure 2a) and 50 min (Figure 2c). This heterogeneity arises, more than likely, from plasticization, where the glassy PVC at the interface is plasticized by the PCL chains which, driven by favorable segmental interactions, diffuse further into the PVC.[8] The penetration of the PCL chains may cause a pressure-driven mechanical deformation process,[35] leading to the formation of heterogeneous structure in the diffusion front. When sufficient PCL segments have diffused into the plasticized PVC layer, individual PVC chains can then diffuse into the rubbery PCL layer. Therefore, as chain diffusion takes place, the width of interfacial regions broadens linearly with time. The diffusion of PCL into glassy PVC is similar to the Case II diffusion seen when a solvent diffuses into a glassy polymer. The major difference here is that the polymer being "dissolved" here, PVC, cannot be taken away from the interface rapidly and gives rise to the observed broadening. A detailed discussion about the nature of the diffusion can be found in the SI (Figure S2).

We also carried out the diffusion process at different annealing temperatures. The results plotted in Figure 4b show an Arrhenius type behavior for the diffusion rate $v = v_0 \exp(-Q/RT)$, where v_0 is the pre-exponential factor, R is the universal gas constant, and T is the diffusion temperature. A value for the apparent activation energy for diffusion, Q, can be calculated from diffusion data at several temperatures. Figure 4b shows this (80, 85, 90, 95, 100, and 105 °C), giving a value for Q of 69.8 kcal/mol for the PVC/PCL system. The value is in the same order of magnitude as that reported previously.[28]

To conclude, we have shown that the nanomechanical mapping of diffusion has high resolution (typical spatial resolution is 5−10 nm, depending on the tip radius and applied forces) to detect large-range diffusion without external labeling and staining, allowing one, based on the Young's modulus maps, to directly quantify diffusion kinetics, evaluate the mechanical property, and observe the microstructure of the interdiffusion regions. These results suggest that nanomechanical mapping of diffusion promises to detect various diffusion behaviors as long as mechanical properties change is involved.

■ ASSOCIATED CONTENT

Supporting Information

Experimental procedures and supporting figures. This material is available free of charge via the Internet at http://pubs.acs.org.

■ AUTHOR INFORMATION

Corresponding Author

*E-mail: wangdthu@wpi-aimr.tohoku.ac.jp.

Notes

The authors declare no competing financial interest.

■ ACKNOWLEDGMENTS

This work was supported by World Premier International Research Center Initiative (WPI), MEXT, Japan. TPR was supported by the US Department of Energy, Office of Basic Energy Science under contract DE-FG02-96ER45612.

■ REFERENCES

(1) Jones, R. A. L.; Klein, J.; Donald, A. M. *Nature* **1986**, *321*, 161−162.

(2) Balke, N.; Jesse, S.; Morozovska, A. N.; Eliseev, E.; Chung, D. W.; Kim, Y.; Adamczyk, L.; García, R. E.; Dudney, N.; Kalinin, S. V. *Nat. Nanotechnol.* **2010**, *5*, 749−754.

(3) Bebensee, F.; Schmid, M.; Steinruck, H. P.; Campbell, C. T.; Gottfried, J. M. *J. Am. Chem. Soc.* **2010**, *132*, 12163−12165.

(4) Capoulade, J.; Wachsmuth, M.; Hufnagel, L.; Knop, M. *Nat. Biotechnol.* **2011**, *29*, 835−842.
(5) Segalman, R. A.; Jacobson, A.; Kramer, E. J.; Lustig, S. R. *Macromolecules* **2004**, *37*, 2613−2617.
(6) Chen, D.; Liu, F.; Wang, C.; Nakahara, A.; Russell, T. P. *Nano Lett.* **2011**, *11*, 2071−2078.
(7) Whitlow, S. J.; Wool, R. P. *Macromolecules* **1991**, *24*, 5926−5938.
(8) Lin, H. C.; Tsai, I. F.; Yang, A. C. M.; Hsu, M. S.; Ling, Y. C. *Macromolecules* **2003**, *36*, 2464−2474.
(9) De Luca, A. C.; Rusciano, G.; Pesce, G.; Caserta, S.; Guido, S.; Sasso, A. *Macromolecules* **2008**, *41*, 5512−5514.
(10) Pampel, A.; Zick, K.; Glauner, H.; Engelke, F. *J. Am. Chem. Soc.* **2004**, *126*, 9534−9535.
(11) Flier, B. M. I.; Baier, M. C.; Huber, J.; Mullen, K.; Mecking, S.; Zumbusch, A.; Woll, D. *J. Am. Chem. Soc.* **2012**, *134*, 480−488.
(12) Zheng, X.; Rafailovich, M. H.; Sokolov, J.; Schwarz, S. A.; Sauer, B. B.; Rubinstein, M. *Phys. Rev. Lett.* **1997**, *79*, 241−244.
(13) Wagner, M. S. *Anal. Chem.* **2005**, *77*, 911−922.
(14) Tomba, J. P.; Carella, J. M.; Pastor, J. M. *Macromolecules* **2009**, *42*, 3565−3572.
(15) Stoffel, N. C.; Dai, C. A.; Kramer, E. J.; Russell, T. P.; Deline, V.; Volksen, W.; Satija, S. *Macromolecules* **1996**, *29*, 6880−6891.
(16) Guvendiren, M.; McSwain, R. L.; Mates, T. E.; Shull, K. R. *Macromolecules* **2010**, *43*, 3392−3398.
(17) Composto, R. J.; Mayer, J. W.; Kramer, E. J.; White, D. M. *Phys. Rev. Lett.* **1986**, *57*, 1312−1315.
(18) Xiao, L. H.; Qiao, Y. X.; He, Y.; Yeung, E. S. *J. Am. Chem. Soc.* **2011**, *133*, 10638−10645.
(19) Yuan, G. C.; Li, C.; Karim, A.; Douglas, J. F.; Han, C. C. *Soft Matter* **2010**, *6*, 2153−2159.
(20) Zhang, J. B.; Lodge, T. P.; Macosko, C. W. *Macromolecules* **2005**, *38*, 6586−6591.
(21) Cappella, B.; Kaliappan, S. K. *Macromolecules* **2006**, *39*, 9243−9252.
(22) Chizhik, S. A.; Huang, Z.; Gorbunov, V. V.; Myshkin, N. K.; Tsukruk, V. V. *Langmuir* **1998**, *14*, 2606−2609.
(23) Wang, D.; Fujinami, S.; Nakajima, K.; Nishi, T. *Macromolecules* **2010**, *43*, 3169−3172.
(24) Sahin, O.; Magonov, S.; Su, C. M.; Quate, C. F.; Solgaard, O. *Nat. Nanotechnol.* **2007**, *2*, 507−514.
(25) Jesse, S.; Kalinin, S. V.; Proksch, R.; Baddorf, A. P.; Rodriguez, B. J. *Nanotechnology* **2007**, *18*, 435503.
(26) Stan, G.; Cook, R. F. *Nanotechnology* **2008**, *19*, 235701.
(27) Wang, D.; Fujinami, S.; Liu, H.; Nakajima, K.; Nishi, T. *Macromolecules* **2010**, *43*, 5521−5523.
(28) Gilmore, P. T.; Falabella, R.; Laurence, R. L. *Macromolecules* **1980**, *13*, 880−883.
(29) Soong, S. Y.; Cohen, R. E.; Boyce, M. C.; Mulliken, A. D. *Macromolecules* **2006**, *39*, 2900−2908.
(30) Derjaguin, B. V.; Muller, V. M.; Toporov, Y. P. *J. Colloid Interface Sci.* **1975**, *53*, 314−326.
(31) Eshraghi, S.; Das, S. *Acta Biomater.* **2010**, *6*, 2467−2476.
(32) Mark, J. E. *Physical Properties of Polymers Handbook*, 2nd ed.; Springer: New York, 2007.
(33) Wang, D.; Liu, Y. H.; Nishi, T.; Nakajima, K. *Appl. Phys. Lett.* **2012**, *100*, 251905.
(34) Butta, H. J.; Cappella, B.; Kappl, M. *Surf. Sci. Rep.* **2005**, *59*, 1−152.
(35) Thomas, N. L.; Windle, A. H. *Polymer* **1982**, *23*, 529−542.
(36) Sauer, B. B.; Walsh, D. J. *Macromolecules* **1991**, *24*, 5948−5955.
(37) Jabbari, E.; Peppas, N. A. *Macromolecules* **1993**, *26*, 2175−2186.